EPJ E
Soft Matter and Biological Physics
EPJ.org
your physics journal

Eur. Phys. J. E (2013) **36**: 16 DOI 10.1140/epje/i2013-13016-1

Experimental study of a vertical column of grains submitted to a series of impulses

G. Lumay, S. Dorbolo, O. Gerasymov and N. Vandewalle

edp sciences Società Italiana di Fisica Springer

Eur. Phys. J. E (2013) **36**: 16
DOI 10.1140/epje/i2013-13016-1

THE EUROPEAN PHYSICAL JOURNAL E

Regular Article

Experimental study of a vertical column of grains submitted to a series of impulses

G. Lumay[1,2], S. Dorbolo[1,2], O. Gerasymov[3], and N. Vandewalle[1,a]

[1] GRASP, Physics Department, University of Liège, B-4000 Liège, Belgium
[2] F.R.S.-FNRS, B-1000 Bruxelles, Belgium
[3] Department of General and Theoretical Physics, Odessa State University of Environment, Ukraine

Received 16 September 2012 and Received in final form 16 January 2013
Published online: 20 February 2013 –

Abstract. We report physical phenomena occurring in a *vertical Newton's cradle* system. A dozen of metallic spheres are placed in a vertical tube. Therefore, the gravity induces a non-uniform pre-compression of the beads and a restoring force. An electromagnetic hammer hits the bottom bead at frequencies tuned between 1 and 14 Hz. The motion of the beads are recorded using a high-speed camera. For low frequencies, the pulses travel through the pile and expel a few beads from the surface. Then, after a few bounces of these beads, the system relaxes to the chain of contacting grains. When the frequency is increased, the number of fluidized beads increases. In the fluidized part of the pile, adjacent beads are bouncing in opposition of phase. This phase locking of the top beads is observed even when the bottom beads experience chaotic motions. While the mechanical energy increases monotically with the bead vertical position, heterogeneous patterns in the kinetic energy distribution are found when the system becomes fluidized.

1 Introduction

Newton's cradle is a classical experiment that is discussed in a large amount of physics textbooks. Moreover, the cradle is also one of the most popular decorative physical toys. Usually, the cradle is composed of 5 suspended identical metallic beads of typically 1 cm of diameter. They have to be very well aligned along the horizontal direction. The distance between two centers should be equal to one diameter. They are suspended by two wires in order to leave them one degree of freedom: they can only move in the vertical plane. The classical experiment consists of releasing one bead. This one collides with the others and one bead is ejected by the other end of the chain. The same experiment is performed when two beads are released, two beads are ejected by the other end. This experiment is used as a paradigm to illustrate the conservation laws. Different variants exist including a cradle with beads of different sizes [1–3]. The collision time measurements have shown that Hertz [4] theory of contacts is of application [5], as observed in the collision of two beads [6].

Despite the relative simplicity of the craddle experiment, the involved subtle mechanisms are far from being trivial. A large number of research works are related to this phenomenon. The propagations of solitary waves have been studied for nearly 450 years. Sen *et al.* have shown in their theoretical reviewing paper [7] that the propagation of single solitary waves in a granular column needs to be re-examined and could lead to exciting technological applications. In engineering science, a column of beads is a good candidate to build shock absorbers and damping systems. Different configurations have been studied [8]: a chain of monodisperse grains, a chain of bidisperse grains and a tapered chain. By applying an external magnetic field on a pile of ferromagnetic grains, an active damping system can be obtained [9]. Indeed, magnetic interactions between the grains modify the physical properties of a granular material [10, 11].

The behavior of the solitary wave is particularly interesting when the column is submitted to gravity due to the non-uniformity of the precompression. The propagation of a solitary wave in a column of grains with a uniform precompression has been analyzed theoretically by Nesterenko [12] and Chatterjee [13] and experimentally studied by Falcon *et al.* [14]. The propagation of a solitary wave in a granular chain submitted to gravity has been solved theoretically by Hong *et al.* [15]. They have shown that the variation of bead compression as a function of the height modifies the propagation of solitary waves. In these studies, all contacts are permanent.

The behavior of a column of beads submitted to mechanical vibrations has also been extensively studied

[a] e-mail: nvandewalle@ulg.ac.be

in the granular material community. Indeed, the agitation induced by vibrations in a packing produces compaction processes [16–20], phase segregations [21], convections [22], granular Leidenfrost effect [23], pattern formation [24, 25], etc. Even the apparently simple system of the single bouncing bead on an oscillating plate leads to interesting behaviors like phase locking and period doubling [26, 27]. Concerning 1D systems, the collision of a column of beads with a fixed wall has been studied by Falcon *et al.* [28]. The behavior of a vertical column submitted to sinusoidal oscillations has been studied by Luding *et al.* [29]. In this study, a progressive transition is observed between a condensed phase, where the beads experience a collective motion, and a fluidized phase, where the bead motion is erratic. The transition between both regimes is controlled by the relative acceleration of the oscillations. In these studies concerning granular materials, the column of beads is submitted to gravity and the top of the column is free. Therefore, the contacts between the grains could be lost.

In this paper, we propose to study a system that is similar to Newton's cradle. It could be nicknamed *vertical Newton's cradle*. It consists of a vertical tube in which identical beads are placed to form a column (see fig. 1). As the beads are loaded by gravity, the contact force between them increases with the height in the column. *Periodical shocks* are given to the bead located at the very bottom of the chain. The top bead being free, the shock wave is able to expel some grains at the top. We tuned the period between two successive shocks in order to study the repartition of the kinetic energy through the sample due to the "interference" between successive shocks.

The vertical Newton's cradle presents several advantages and specificities. i) The expelled grains (located at the top of the chain) in our system are submitted to the gravity force mg. That situation contrasts sharply with Newton's cradle for which the expelled grains are submitted to a reduced gravity force $mg\sin(\alpha)$, where α is the angle between the pendulum and the vertical, whose angle is small. As a consequence, in the vertical cradle, the forces which tend to reset the system to equilibrium are large compared to the horizontal cradle. ii) The propagation of a shock though a line of beads has been intensively studied as reminded in this introduction. In addition, a lot of works and studies can be found on sinusoidal excitation of a column. In our system, we combine the physics related to the shock (propagation, rapid relaxation) to the physics related to the periodical excitation (fluidization). We will see that, even if our system presents similarities with the oscillating column, the behavior of the *vertical Newton's cradle* is different. We also compare our experimental results with theoretical works dedicated to the modeling of the vertical loaded chain.

In sect. 2, the experimental set-up is described. Section 3 is devoted to the analysis of the different bead trajectories. From the measurement of the bead positions, several parameters will be particularly studied to emphasize the physical complexity of the system. From the bead trajectories, phase locking will be pointed out. Afterward, the motion of the center of mass is analyzed and the average energy as a function of the bead number is measured. In sect. 4, the results are discussed and compared with theoretical models. Finally, the conclusions are drawn in sect. 5.

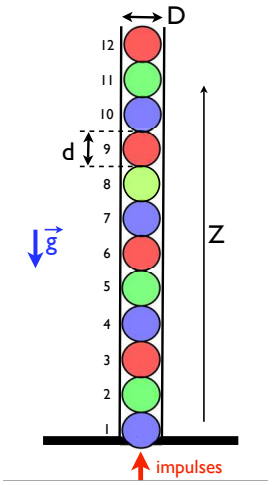

Fig. 1. (Color online) Sketch of the experimental set-up at rest. Twelve beads are placed in a vertical tude of inner diameter D. The diameter of a bead is d. Bead numbers are illustrated. Taps (impulses) are applied from the bottom and bead trajectories are tracked by a camera.

2 Experimental set-up

Figure 1 presents a sketch of our experimental set-up. Twelve metallic beads are placed in a vertical glass tube. The diameter and the mass of the stainless steel beads are respectively $d = 8.73\,\text{mm}$ and $m = 2.74\,\text{g}$. The inner diameter of the tube ($D = 8.9\,\text{mm}$) is slightly larger than the bead diameter. The bottom bead is blocked by a ring. Therefore, this bead can be hit by an electromagnetic hammer which injects impulses in the column. The frequency and the intensity of the impulses are controlled by a micro-controller. The frequency can be adjusted between 1 and 14 Hz. The impulsion provided by the hammer at each tap is 0.16 kg m/s. The typical duration of the collision between the bottom bead and the hammer is at most 1 ms. A high-speed camera is used to record the motion of the grains. Lighting is ensured by a lamp located far away from the beads in order to have a spot on each bead, providing bead positions on the images. Afterward, the motion of the beads are obtained with a classical tracking method. The beads are numbered from bottom (1) to top (12).

3 Results

Figure 2 presents typical trajectories of the beads for three selected values of the excitation frequency (1.4, 7.2 and 13.8 Hz). The equilibrium positions of the beads have been substracted from their vertical positions Z_i to obtain the

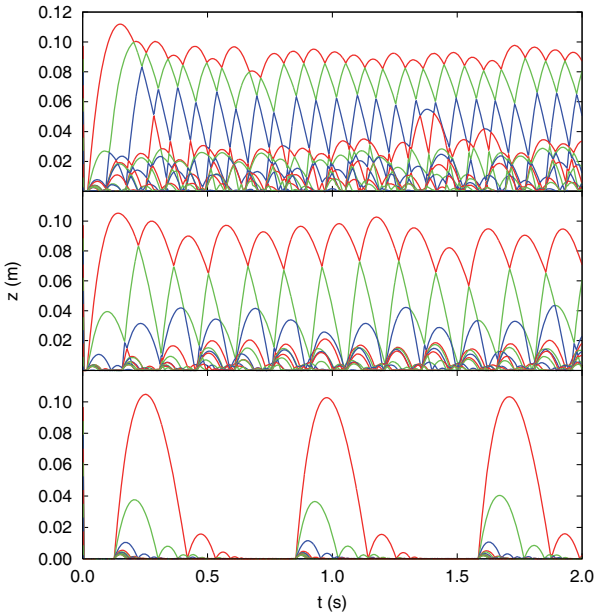

Fig. 2. (Color online) Trajectories of the twelve beads for three values of the excitation frequency. From bottom to top, the frequencies are, respectively, 1.4, 7.2 and 13.8 Hz. The height of the beads when the column is at rest has been subtracted from the trajectories.

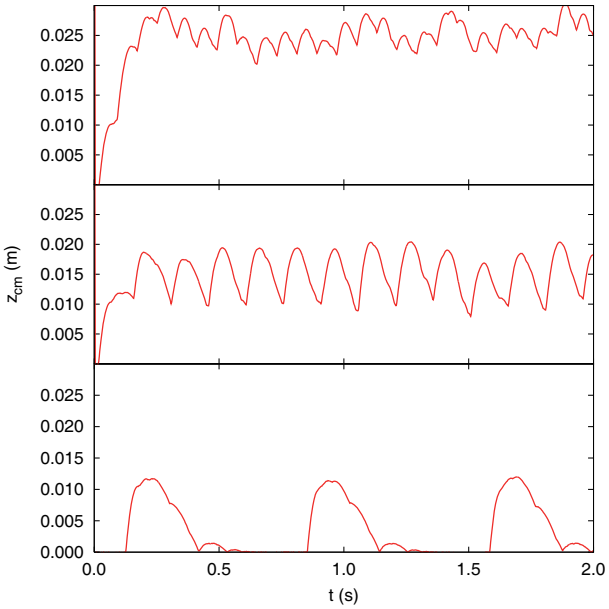

Fig. 3. (Color online) Displacement of the center of mass $z_{\rm cm}$ as a function of time, for three different excitation frequencies. From bottom to top, $f = 1.4$, 7.2 and 13.8 Hz.

displacements z_i of the bead number i given by

$$z_i = Z_i - \left[id - \sum_{k=1}^{i} \epsilon_k \right], \qquad (1)$$

where ϵ_k is the overlapping at the contact below the bead k. The deformation ϵ_k of the beads can be estimated. From the Rockwell hardness scale [30] given by the bead manufacturer, the deformation at the bottom of the column due to gravity load is roughly $\epsilon_k \simeq 7 \cdot 10^{-9}$ m. From Hertz's law (see eq. (6)), it is possible to determine this deformation using the Young modulus of stainless steel. We found a similar value: $\epsilon_k \simeq 10^{-8}$ m. Both estimates are far below the resolution of our instruments. Nevertheless, the equilibrium position of each grain is determined before the experiment.

First, let us describe the motions experienced by the beads due to a single tap. The behavior is seen at very low frequency (bottom plot of fig. 2). All the beads start to move directly after the impulse according to the resolution of the high-speed camera (1/500 s). The nine bottom beads move together and behave like a single block. This body experiences a small parabolic motion before coming back to the equilibrium position. Only one parabola is observed; no bouncing occurs according to the spatial resolution of our measurements. We conclude that the block behaves like a complete inelastic body. The impulse is transmitted through this block to the three top beads. The beads number 10, 11 and 12 take off and lose the contact with their neighbors. Their trajectories are also parabolas with an amplitude that increases with the number of the bead. Moreover, these beads bounce before coming back to their equilibrium state. The same scheme is repeated for every tap.

The dissipation due to the tube walls may be estimated by analyzing the motion of the top bead. While flying, the bead experiences a parabolic trajectory. Assuming a free-falling motion, the acceleration should be found equal to gravity. The fit of the parabola provides an acceleration of about 9.77 m/s^2. This is close to the gravity constant acceleration, meaning that friction is low.

If the tap frequency f increases, *i.e.* if the period $\mathcal{T} = 1/f$ between two successive impulses decreases, the behavior of the pile becomes strongly different. Indeed, successive pulses interact inside the column. As shown in fig. 2, the number of fluidized beads increases with the impulses frequency f and the rest of the column still behaves like a single block. In the fluidized part of the pile, adjacent beads bounce in opposition of phase. This phase locking of the top beads is observed even when the bottom beads experience chaotic motions (see fig. 2 (top)).

Figure 3 shows the temporal evolution of the position of the center of mass $z_{\rm cm}$ given by

$$z_{\rm cm} = \frac{1}{12} \sum_{i=1}^{12} z_i. \qquad (2)$$

After a short transient regime, the center of mass is found to oscillate around a median value which increases with the tap frequency f. Figure 4 presents three main characteristics of $z_{\rm cm}$ as a function of f. The average of $z_{\rm cm}$ over several periods is seen to increase linearily with the tap frequency (see fig. 4 (top)). However, the minimum value of $z_{\rm cm}$ starts to grow after a threshold frequency, meaning that at least one bead is always detached from the column (see fig. 4 (center)). Finally, the amplitude of the $z_{\rm cm}$ oscillations decreases when the tap frequency increases.

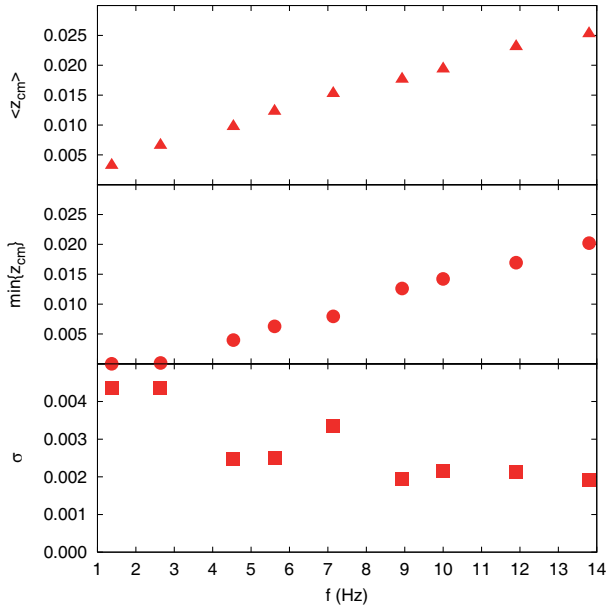

Fig. 4. (Color online) Three main characteristics of the average motion of the beads ($z_{\rm cm}$) as a function of the tap frequency f. From top to bottom, the figure presents the average position of the column $\langle z_{\rm cm}\rangle$, the minimum value of $z_{\rm cm}(t)$ and the fluctuations of the average position $\sqrt{\langle z_{\rm cm}^2\rangle - \langle z_{\rm cm}\rangle^2}$.

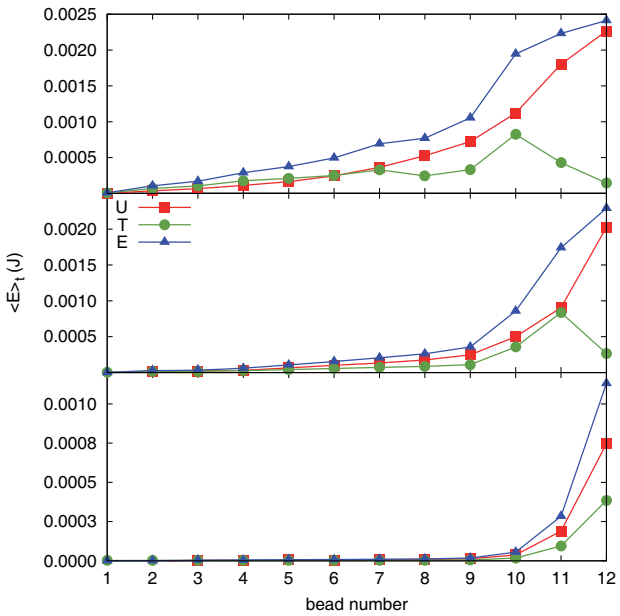

Fig. 5. (Color online) Energies averaged over several periods as a function of the bead number. T (circles), U (squares) and E (triangles) are respectively the kinetic, the potential and the total energy. From top to bottom, the excitation frequencies are, respectively, 1.4, 7.2 and 13.8 Hz.

Since the standard deviation of the center of mass (see fig. 4 (bottom)) is reduced at high frequency, more collisions per time unit between the beads are expected and consequently more energy exchanges. When the frequency is high, one observes indeed that the separation between beads increases (see fig. 2) implying individual motion instead of block motion.

The energy of each bead has been calculated from the knowledge of the normalized trajectories $z_i(t)$, where $i = \{1, \ldots, 12\}$ is the bead number. The kinetic energy is therefore given by

$$T_i(t) = \frac{1}{2} m \left(\frac{z_i(t + \Delta t) - z_i(t)}{\Delta t} \right)^2, \qquad (3)$$

where m is the mass of each bead and $\Delta t = 2\,\text{ms}$ is the time between two successive frames. The variation of potential energy is given by

$$\Delta U_i(t) = m g z_i(t). \qquad (4)$$

Since the equilibrium positions of the beads are not taken into account in the normalized positions $z_i(t)$, the value of this potential energy is zero when the column is at rest. The total mechanical energy E_i is the sum of T_i and U_i. Figure 5 presents the energies averaged over several periods as a function of the bead number. For low values of the tap frequency (see fig. 5 (bottom)) below the onset of fluidization, both kinetic and potential energies increase monotonicaly with the bead number i. Moreover, the value of the total energy is almost zero for the nine lowest beads. A large block is still present in the system. When the applied frequency f becomes higher (see fig. 5 middle and top), the energy is distributed over a larger number of beads and the kinetic energy T shows a maximum which goes down inside the pile when f increases.

4 Discussion

For low tap frequencies, the pulses travel along the column and expel some grains at the top. The bottom part of the column experiences a small parabolic flight as a single block. After the tap, the system dissipates the energy when the flying grains are bouncing on the column. We define a flying time τ_i which is the duration of the first parabolic flight experienced by the bead number i. After a single tap, we have $\tau_i = \tau_{i+1} = 0.064\,\text{s}$ for $i < 10$ and $\tau_{10} = 0.096\,\text{s} < \tau_{11} = 0.176\,\text{s} < \tau_{12} = 0.291\,\text{s}$. The relaxation time for the whole column is about $\tau_r \approx 0.4\,\text{s}$.

If the tap frequency f increases, *i.e.* if the period $\mathcal{T} = 1/f$ between two successive impulses decreases below τ_r, successive pulses interact inside the column. If $\tau_{12} > \mathcal{T} > \tau_{11}$, the second impulse occurs between the end of the parabolic flight experienced by the bead number 12 and the end of the parabolic flight experienced by the bead number 11. Then, bead 11 is ejected from the column and collides with bead 12. As a consequence, the beads located at the top are fluidized while the rest of the column still behaves like a single block. The phase locking and the ordered character of the beads motion is related to the method of injection of the energy in the system. Indeed, this effect was not observed in the case of a pile submitted to sinusoidal oscillations [29]. In our system, the bottom block transmits the impulses to the top beads

which experience a phase locking while the energy is more distributed over the whole pile in the case of sinusoidal oscillations. The existence of the bottom block is allowed because the system has the possibility to relax between two taps while the plate is always in motion in the oscillating configuration. When $\tau_{11} > \mathcal{T} > \tau_{10}$, the same arguments demonstrate that the top three beads are fluidized. Finally, if period $\mathcal{T}$ becomes lower than τ_{10} the block of the nine bottom beads described previously is more and more decomposed. The fluidized part of the pile reminds of the Tonks gas that consists of a one-dimensional gas of hard spheres [31].

Concerning the distribution of energy in the column, one could expect that for a fluidized bed, both kinetic and potential energies grow with bead number. Indeed, at first glance, the beads located at the top of the column are submitted to a smallest confinement pressure and have the ability to move more freely. However, at high frequency (see fig. 5), the surprising result is that the maximum of the kinetic energy is not located at the position of the top bead but is located at bead number $i = 10$! It seems that an increases of f involves a shift of this peak towards low i values. In fig. 2, a careful observation of trajectories at high frequency shows indeed that the bead $i = 10$ has the largest amplitude, while the top bead has a limited motion. This localization of high kinetic energy inside the column was not expected and looks similar to a Leidenfrost effect [23].

The coexistence of a condensed and a fluidized phase complicates the modeling of the system. The condensed phase can be modeled by a vertical column of non-linear oscillators. Considering the equation which governs the motion of mechanical impulse impacted from the bottom of the vertical granular cradle with Hertzian contacts (or non-linear spring), one has

$$\frac{\mathrm{d}^2 Z_i}{\mathrm{d}t^2} = \gamma \left\{ [d - (Z_i - Z_{i-1})]^{\frac{3}{2}} - [d - (Z_{i+1} - Z_i)]^{\frac{3}{2}} \right\} + g \tag{5}$$

for each bead i except the last one which has only one contact. The parameter $\gamma = E/3(1-\nu^2)m$ takes into account the Young elastic modulus E, the Poisson ratio ν, and the mass m of each particle. The equilibrium condition for every bead k reads

$$g\, k = \gamma\, \epsilon_k^{\frac{3}{2}} \tag{6}$$

that one can use also in eq. (1). One may note that in this model governed by eq. (5), both friction or non-elasticity effects are neglected. This belongs to Hertzian contacts approximation. Under the assumption of weak non-linearities, *i.e.* $\epsilon_k < 1$, eq. (5) can be mapped into functional-differential equations [32] which have a rigourous solution given by Bessel functions J_{2i} of an integer order, *i.e.*

$$z_i = J_{2i}\left(g^{\frac{1}{6}} \gamma^{\frac{1}{3}} t \right), \tag{7}$$

defining a characteristic time

$$\tau = g^{-\frac{1}{6}} \gamma^{-\frac{1}{3}}. \tag{8}$$

For the beads used in this experiment, the obtained characteristic time is $\tau \approx 10\,\mu$s. Therefore, the fact that we do not measure any time delay between the impulses on the chain and the top grains expelled with our time resolution is coherent with this model.

Of course, any observable bead motion should be described in form of a linear combination of a few cylindrical waves which should take into account boundary conditions. The remarkable feature of this simple model is that oscillations are predicted and more importantly their amplitude depends on the integer order of cylindrical waves. Hong *et al.* have shown with a similar model that, due to the gravitational compaction of the column, the impulses propagate dispersively. Therefore the pulses do not stay a soliton during the propagation, in contrary to the propagation mode in a horizontal column. This dispersive propagation explains that more than one bead is expelled from the column after an impulse.

Concerning the fluidized part of the system, the ballistic motion of beads has already been studied theoretically by Gerasymov *et al.* [33]. This one-dimensional model, considering inelastic particles in the case of the simplest modes of external energy supply, allows the possibility for stationary states, which correspond to simple periodic motions. This result is in agreement with our remarkable observation of phase locking in the fluidized part of the column. The phase locking is a common feature shared by bouncing ball systems [27,34,35] such as a single bead in an oscillating box. Numerical models could therefore be implemented for describing the fluidized part but this remains outside the scope of the present paper.

In [29], the bead column is sinusoidally excited, leading to fluidization above some acceleration threshold. This transition is due to the take-off and subsequent bounces of the column above the threshold. Herein, the excitation is discontinuous and the amount of energy injected in the column (within one tap) is fixed. We have found a similar threshold linked to the competition between dissipation rate and frequency. Contrary to [29], the beads separate into two parts: a static block at the bottom of the column above which moving grains are freely falling and colliding. The distribution in kinetic energy is therefore completely different if one considers continuous energy injection or taps.

5 Conclusion

A vertical column of twelve beads has been excited by a hammer that hits the bottom of the column at a given frequency f. Due to the gravity, the beads are submitted to a non-uniform compression. The system is dissipative and the contact force is non-linear. The top bead being free, the shock wave is able to expel some grains at the top. The dynamics of this system is found to be rich. For low values of the applied frequency ($f < f_0$), only a few beads situated at the top of the pile are performing successive parabolic flights. A part of the system remains in a "condensed" phase while the second part is fluidized. When the frequency increases above the onset for fluidization,

all beads are in motion. Adjacent beads are bouncing in opposition of phase. This phase locking and the ordered character of the beads motion is related to the method of injection of the energy in the system. Indeed the behavior of our pile is radically different from the case of a sinusoidal excitation [29]. The average energy of each bead has been calculated. The kinetic energy presents a maximum which was unexpected. This maximum goes down inside the pile when the frequency increases and could lead to a Leidenfrost effect for higher values of the injection frequency.

SD, OG and GL would like to thank F.R.S.-FNRS for financial support. This work has been also supported by INANOMAT project (IAP P6/17) of the Belgian Science Policy.

References

1. F. Herrmann, M. Seitz, Am. J. Phys. **50**, 977 (1982).
2. M. Reinsch, Am. J. Phys. **62**, 271 (1993).
3. S. Hutzler, G. Delaney, D. Weaire, Finn MacLeod, Am. J. Phys. **72**, 1508 (2004).
4. H. Hertz, J. Reine. Angew. Math. **92**, 156 (1881).
5. D.R. Lovett, K.M. Moulding, S. Anketell-Jones, Eur. J. Phys. **9**, 323 (1998).
6. B. Leroy, Am. J. Phys. **53**, 346 (1985).
7. S. Sen, J. Hong, J. Bang, E. Avalos, R. Doney, Phys. Rep. **462**, 21 (2008).
8. R.L. Doney, J.H. Agui, S. Sen, J. Appl. Phys. **106**, 064905 (2009).
9. B.M. Shah, J.J. Nudell, K.R. Kao, L.M. Keer, Q.J. Wang, K. Zhou, J. Sound Vibration **330**, 182 (2011).
10. G. Lumay, S. Dorbolo, N. Vandewalle, Phys. Rev. E **80**, 041302 (2009).
11. G. Lumay, N. Vandewalle, Phys. Rev. E **82**, 040301 (2010).
12. V.F. Nesterenko, J. Appl. Mech. Tech. Phys. **24**, 733 (1983).
13. A. Chatterjee, Phys. Rev. E **59**, 5912 (1999).
14. C. Coste, E. Falcon, S. Fauve, Phys. Rev. E **56**, 6104 (1997).
15. J. Hong, J.-Y. Ji, H. Kim, Phys. Rev. Lett. **82**, 3058 (1999).
16. J.B. Knight, C.G. Fandrich, Chun Ning Lau, H.M. Jaeger, S.R. Nagel, Phys. Rev. E **51**, 3957 (1995).
17. P. Richard, M. Nicodemi, R. Delannay, P. Ribière, D. Bideau, Nat. Mater. **4**, 121 (2005).
18. G. Lumay, N. Vandewalle, Phys. Rev. Lett. **95**, 028002 (2005).
19. F. Ludewig, S. Dorbolo, N. Vandewalle, Phys. Rev. E **70**, 051304 (2004).
20. J.E. Fiscina, G. Lumay, F. Ludewig, N. Vandewalle, Phys. Rev. Lett. **105**, 048001 (2010).
21. A. Kudrolli, Rep. Prog. Phys. **67**, 209 (2004).
22. A. Garcimartin, D. Maza, J.L. Ilquimiche, I. Zuriguel, Phys. Rev. E **65**, 031303 (2002).
23. P. Eshuis, K. van der Weele, D. van der Meer, D. Lohse, Phys. Rev. Lett. **95**, 258001 (2005).
24. E. Cément, L. Vanel, J. Rajchenbach, J. Duran, Phys. Rev. E **53**, 2972 (1996).
25. E. Clément, L. Labous, Phys. Rev. E **62**, 8314 (2000).
26. J.C. Géminard, C. Laroche, Phys. Rev. E **68**, 031305 (2003).
27. T. Gilet, N. Vandewalle, S. Dorbolo, Phys. Rev. E **79**, 055201R (2009).
28. E. Falcon, C. Laroche, S. Fauve, C. Coste, Eur. Phys. J. B **5**, 111 (1998).
29. S. Luding, E. Clément, A. Blumen, J. Rajchenbach, J. Duran, Phys. Rev. E **49**, 1634 (1994).
30. W.F. Smith, J. Hashemi, in *Foundations of Material Science and Engineering*, 4th edition (McGraw-Hill, 2001).
31. L. Tonks, Phys. Rev. **50**, 955 (1936).
32. E. Pinney, *Ordinary Difference-Differential Equations* (University of California Press, Berkley and Los Angeles, 1955).
33. O.I. Gerasymov, N. Vandewalle, G. Lumay, S. Dorbolo, A. Spivak, Ukr. J. Phys. **53**, 1128 (2008).
34. N.B. Tufillaro, T. Abbott, J.P. Reilly, *An experimental approach to non linear dynamics and chaos* (Addison-Wesley, Reading, MA, 1992).
35. D. Terwagne, T. Gilet, N. Vandewalle, S. Dorbolo, Langmuir **26**, 11680 (2010).